

Polymer gel electrolytes synthesized by photopolymerization in the presence of star-shaped oligo(ethylene glycol) ethers (OEGE)

K. Edlmann*, B. Sandner

Institut für Technische und Makromolekulare Chemie, Fachbereich Chemie, Martin-Luther-Universität Halle-Wittenberg, D-06099 Halle (Saale), Germany

Received 1 April 2004; received in revised form 25 June 2004; accepted 22 July 2004

Available online 2 December 2004

Abstract

The photoinitiated cross-linking polymerization of tri(ethylene glycol) dimethacrylate and its copolymerization with cyanomethyl methacrylate in the presence of LiCF_3SO_3 and of various oligo(ethylene glycol) methyl ethers as plasticizer was studied for potential use of the resulting polymer gel electrolytes in lithium batteries. Comparing linear and star-shaped (three and four arm molecules) oligo(ethylene glycol) methyl ethers, the influence of the architecture of the plasticizers on the polymerization course was investigated by means of differential scanning calorimetry. Linear and star-shaped plasticizers with molar masses < 1000 g/mol differ from each other concerning the dependence of their viscosity on their molar mass but not concerning the influence of the viscosity on the polymerization rate. Compared with linear plasticizers, the star-shaped ones have as an essential advantage a distinctly lower tendency to crystallize which is even completely suppressed in some cases. The gels were characterized with regard to the network density of their polymer matrix, to their thermal transitions, thermo-mechanical properties and ionic conductivity. The conductivity of solutions and gels with star-shaped plasticizers was slightly lower than that with linear ones at temperatures above room temperature.

© 2004 Published by Elsevier Ltd.

Keywords: Oligo (ethylene glycol) ethers; Photopolymerization; Polymer gel electrolyte

1. Introduction

The photoinitiated free-radical polymerization of various monomers in the presence of a lithium salt and a solvent or plasticizer proved as an appropriate method to prepare directly applicable films of polymer gel electrolytes for the potential use in lithium batteries [1–8]. The films may be produced by this method with a significantly less expenditure of time compared with films commonly obtained by solvent casting. In the latter case, only soluble polymers are applicable to form the gel electrolyte films. Their thermal stability and with that their shape resistance may be low. In contrast to this, cross-linking monomers can be photopolymerized yielding gel electrolyte films of highly thermal and mechanical stability because of the cross-linked structure of the polymer matrix.

Poly(ethylene glycol) is the unique solvating polymer for an extremely wide range of metal salts. Therefore, both cross-linking monomers and plasticizers including segments of oligo(ethylene glycol) (EG_n) have been studied as components for gel electrolyte films [4–10].

Earlier, we reported the preparation of gel electrolyte films by photoinitiated polymerization of oligo(ethylene glycol) dimethacrylates (EG_nDMA) with $n=3, 9$ and 23 in the presence of oligo(ethylene glycol) dimethylethers (EG_nDME) with $n=4$ and 11 and of LiCF_3SO_3 as the ion conducting salt [6]. Only the highly cross-linked networks from EG_3DMA yielded gel electrolyte films of appropriate mechanical stability, also at high contents of plasticizer, e.g. 75 wt%. The films had a heterogeneous structure exhibiting separate glass transitions of the polymer and of the solution of the salt in the plasticizer. EG_{11}DME rendered, especially advantageously as a plasticizer relating to the polymerization rate (strong gel effect owing to its high viscosity) and the mechanical as well as electrochemical stability of the gel electrolytes compared to gels containing EG_4DME . On the

* Corresponding author. Tel.: +49-3461-4621-78; fax: +49-3461-4621-73

E-mail address: edlmann@chemie.uni-halle.de (K. Edlmann).

other hand, the low viscosity of the latter brings about a higher mobility of the ions and with that a higher ionic conductivity.

The content of free ions of the system can be increased by introduction of polar groups both into the polymer [4–7] and the plasticizer [9]. It has been shown, that the cationic transference numbers and the electrochemical stability of the gel electrolytes will be higher if the polymer include the polar groups and the plasticizer a sufficient number of EG units for the optimum solvation and transport of Li^+ cations. However, the mobility of the latter and of EG_{11}DME is restricted already at room temperature due to the high tendency to crystallization of this plasticizer [6].

Therefore, we prepared three arm (OEGE-3) and four arm (OEGE-4) oligo(ethylene glycol) methyl ethers of various molecular weights (Scheme 1) as a new type of plasticizer with the expectation that their viscosity and their tendency to crystallization may be reduced compared with those of linear EG_nDME of similar molecular weight. The use of star-shaped OEGE with three and four arms as a plasticizer for gel electrolytes has already been proposed in [11].

Since the viscosity of the plasticizer influences the course of the free-radical polymerization and with that the properties of the resulting gel electrolyte, we investigated the photoinitiated homopolymerization of EG_3DMA and its

copolymerization with cyanomethyl methacrylate (CyMA) (Scheme 1) as a polar comonomer in the presence of linear and star-shaped plasticizers and of the ion conducting salt LiCF_3SO_3 . The polymerization rate was monitored by means of differential scanning calorimetry (DSC). The viscosity and thermal properties of solutions of the salt in these plasticizers as well as the thermo-mechanical properties and the ionic conductivity of the corresponding gel electrolytes are reported.

2. Experimental part

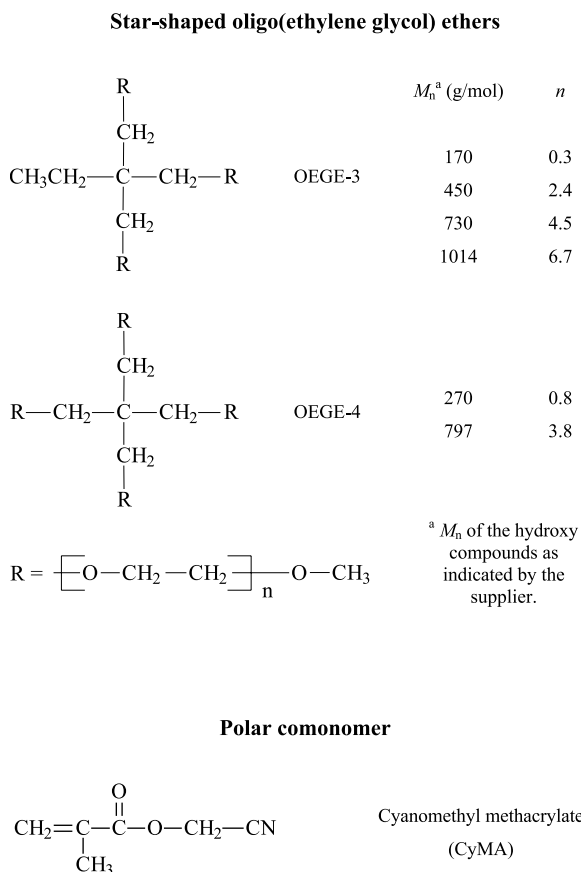
2.1. Materials

The linear oligo(ethylene glycol) dimethyl ethers EG_3DME , EG_4DME , $\text{EG}_{5-6}\text{DME}$ and EG_{11}DME were purchased from Merck and EG_3DMA from Aldrich, and they were dried over molsieves 4 \AA . The photoinitiator Lucirin TPO (2,4,6-trimethylbenzoyldiphenylphosphineoxide) was purchased from the BASF AG. LiCF_3SO_3 (Fluka) was dried in vacuum at $120 \text{ }^\circ\text{C}$ for 24 h. Dioxane, toluene, hexane and acetone were distilled.

Cyanomethyl methacrylate (CyMA) was prepared according to a procedure described by Ueda et al. [12] by the reaction of chloroacetonitrile and methacrylic acid in the presence of triethyl amine.

2.2. Synthesis of star-shaped OEGE

Three arm OEGE were synthesized from trimethylolpropane ethoxylates (TMPE) (Aldrich) ($M_n = 170, 450, 730$ and 1014 g/mol , respectively) and four arm OEGE from pentaerythrit ethoxylates (PEE) (Aldrich) ($M_n = 270$ and 797 g/mol) by methylation of the hydroxyl end groups. An example is given as follows: 50 g trimethylolpropane ethoxylate with $M_n = 730 \text{ g/mol}$ (TMPE 730) (68.5 mmol), 17.3 g potassium hydroxide powder (0.308 mol) (Merck), 12.5 mg 2,6-di-*tert*-butyl-4-methylphenol ($5.67 \times 10^{-2} \text{ mmol}$) and 100 ml dioxane were charged into a three necked round-bottom flask, then stirred and refluxed for 1 h under an argon atmosphere. Then 43.8 g methyl iodide (0.308 mol) (Merck) were added slowly, and the mixture was refluxed with continuous stirring for 5 h. After cooling to room temperature the solution containing the product was filtered from the precipitated potassium iodide. Then dioxane and the excess of methyl iodide were removed in vacuum, and the product was decanted from the precipitate formed again. In this way, only conversions of 80–90% of the OH groups were reached as found by IR and ^1H NMR spectroscopy. Therefore, the isolated product was reacted again with 2.3 g potassium hydroxide (41.1 mmol) and 5.8 g methyl iodide (41.1 mmol) in 100 ml dioxane in the same procedure described above to convert the residual OH groups. After filtering the solution, dioxane and the excess of methyl iodide were removed in vacuum. The product was



Scheme 1.

extracted with toluene (only the product from TMPE 450 was extracted with hexane), then the solvent was removed in vacuum. The residue was dissolved in acetone and eluted with acetone over a silicagel-filled column. Then acetone was removed in vacuum. In the case of the products of TMPE 450, 730, 1014 and PEE 797 (OEGE-3 450, 730, 1014 and OEGE-4 797), conversions of the hydroxyl groups of >95% were reached as found by IR and ^1H NMR spectroscopy (yields: 40–50, 80% in the case of OEGE-3 1014). OEGE-3 170 and OEGE-4 270 could be isolated by distillation in vacuum directly after removing of dioxane and methyl iodide (OEGE-3 170: $\text{bp}_5 = 75\text{--}125\text{ }^\circ\text{C}$, yield: 60%, OEGE-4 270: $\text{bp}_5 = 70\text{--}190\text{ }^\circ\text{C}$, yield: 42%). Unreacted hydroxyl groups were not detected by IR and ^1H NMR spectroscopy. The OEGE were stored over a mixture of molsieves 4 Å and Al_2O_3 (OEGE-3 170 only over molsieves 4 Å) in an argon filled box.

2.3. Membrane preparation

A mixture of the monomers including 2 mol% of the initiator Lucirin TPO, the plasticizer and the ion conducting salt (see Results and discussion for detailed monomer ratio and contents of plasticizer and salt) was irradiated with UV light (lamp: Dr. Benda Laborgeräte UV-Strahler NU-8, emitted UV light at wavelengths of 254 and 366 nm, distance: 10 cm) at room temperature for 15 min in an argon filled glove box. All samples were annealed at $80\text{ }^\circ\text{C}$ for 8 h to complete the conversion of the monomers.

2.4. Sol–gel analysis

For the determination of the sol and gel content, nearly 0.2 g of the samples were extracted three times with 5 ml chloroform, dried in vacuum at $80\text{ }^\circ\text{C}$ and then weighed. The salt was not soluble in the solvent. Therefore, only insignificant amounts of salt could be extracted. To identify non-reacted monomer, the sol was isolated by evaporation of the solvent from the obtained solution and analyzed by ^1H NMR spectroscopy.

2.5. Raman spectroscopy

Raman spectra were obtained using a Bruker Fourier transform infrared spectrometer IFS 66 equipped with the Raman module FRA 106 (Nd-YAG diode laser, 300 mW). The C=C stretching band (1639 cm^{-1}) of the monomers was analyzed to calculate the residual content of C=C double bonds in the copolymer networks.

2.6. IR spectroscopy

IR spectra were obtained using a Bruker Fourier transform infrared spectrometer IFS 66 equipped with a Nd-YAG diode laser (300 mW). The OH band of star-shaped oligo(ethylene glycol)s (between 3400 and

3500 cm^{-1}) was analyzed to calculate the conversion of the hydroxyl groups.

2.7. ^1H NMR spectroscopy

High-resolution ^1H NMR spectra of samples dissolved in CDCl_3 were obtained using a Varian 300 MHz spectrometer. The signal of the methylene group linked to the OH group (3.7 ppm) of TMPE and PEE was analyzed to calculate the conversion of the hydroxyl groups reached by the methylation reaction. To identify non-reacted monomer in the sols, the CH_2 signals of the methacryl groups of the monomers ($\delta = 5.5, 6.1\text{ ppm}$) were analyzed.

2.8. Differential scanning calorimetry

The photopolymerizations were monitored using the differential scanning calorimeter DSC 220C (Seiko Instruments Inc.) equipped with a Hg–He lamp (emitted UV light in the range of wavelengths of 250–500 nm). The monomer mixture (30–40 mg) was dropped into an aluminium pan and then put onto the sample holder. A second pan containing an equally compositioned, completely polymerized sample as a reference material was placed on the reference holder. The reaction was started by irradiation after thermal equilibration at $30\text{ }^\circ\text{C}$ for 60 s under anaerobic conditions.

The conversion of the C=C double bonds was determined from the obtained polymerization heat using a polymerization enthalpy (ΔH_p) of 55 kJ/mol as a reference value, which has been published for methyl methacrylate at $25\text{ }^\circ\text{C}$ [13], and approximately for CyMA [14] and oligo(ethylene glycol) methacrylates [14,15].

Thermal transitions of the gel electrolytes were monitored by use of the DSC 220C with a heating rate of 10 K/min.

2.9. DMA measurements

Dynamic mechanical measurements were performed using a Netzsch DMA 242/1/F at the compression modulus with a limit dynamic force of 6 N, a frequency of 1 Hz and a heating rate of 3 K/min. Samples with a diameter of 10 mm and a height of 1–2 mm were used. For determination of the molecular weight M_c of the chains between the network junction points, samples completely extracted with chloroform were used. M_c was calculated from the dynamic storage modulus E' measured at a temperature $T = T_g + 50\text{ K}$ as described previously [6].

2.10. Viscosity

Measurements of the viscosity of LiCF_3SO_3 containing OEGE solutions were carried out using a rotation viscosimeter Physica Os 300 at a temperature of $20\text{ }^\circ\text{C}$. The viscosity of the solution of OEGE-3 1014 with LiCF_3SO_3

decreased initially with the rotation time of the viscosimeter and was therefore determined after 1 min.

2.11. Ionic conductivity

The ionic conductivity of LiCF_3SO_3 solutions in OEGE were obtained using the Knick conductometer Portamess[®] 911 Cond equipped with a four pole electrode with integrated Pt 1000 temperature sensor.

Measurements of the conductivity of the gels were carried out on nearly 100 μm thick films by means of a combination of a Potentiostat/Galvanostat (model 263 A) and a frequency response analyzer (model 1025) from EG&G in a frequency range from 10 to 10^5 Hz using stainless steel electrodes.

3. Results and discussion

3.1. Viscosity and thermal transitions of star-shaped OEGE

It is known that the viscosity of a monodisperse star-shaped polymer in the melt is not proportional to the total molecular weight M of the whole molecule but only to the molecular weight M_a of an arm, and η depends exponentially on M [16]. Consequently, LiCF_3SO_3 solutions of star-shaped OEGE were expected to exhibit possibly higher ionic conductivities than linear ones caused by a higher mobility of the star molecules and thus, of the ions.

As can be seen in Fig. 1a, decreased viscosities were determined for star-shaped OEGE in comparison to linear OEGE. These differences are only slightly for three arm OEGE.

Fig. 1b shows η as a function of the span molecular weight M_s , which is equal to the total molecular weight of a linear molecule or to twice the arm molecular weight of a star molecule, $M_s = 2M_a$. In the case of linear OEGE, η depends on the molecular weight M according to the relationship $\eta \sim M^a$, with $a = 1.9$. It is visible from the Fig. 1a and b that this η - M relationship is not valid for the star-shaped ethers, because their viscosity correlates with M_a (and M_s , respectively) (Fig. 1b) indeed, and an exponent of M_a of 2.5 was found in this case.

The viscosity of solutions of LiCF_3SO_3 in the star-shaped and also in the linear OEGE is higher than that of the corresponding pure ethers (Fig. 1). In contrast to the pure star-shaped ethers, their solutions with LiCF_3SO_3 do not exhibit lower viscosities than solutions in linear ethers (Fig. 1a) with comparable molecular weight. However, for the solutions in star-shaped OEGE (Fig. 1b), η depends on M_a with a lower exponent of 1.9 compared with an exponent of 2.6 for the solutions in linear OEGE.

Exceptions are generally OEGE-3 1014 and its solution with LiCF_3SO_3 , having viscosities distinctly higher than expected. Probably, the critical molecular weight M_{crit} has been attained where η of star-shaped polymers increases

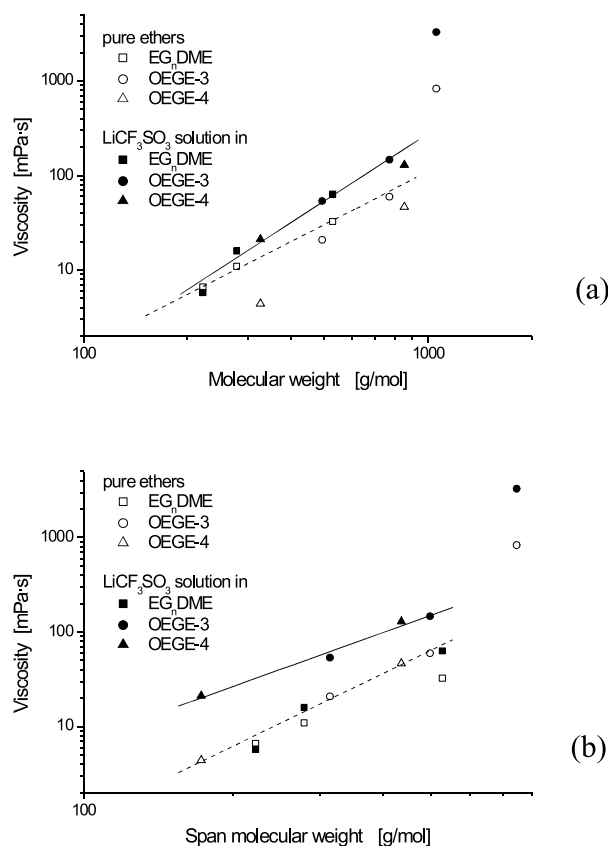


Fig. 1. Viscosity η of linear and star-shaped OEGE and of their solutions with 0.55 mol/kg LiCF_3SO_3 in dependence on the molecular weight of the ether at 20 °C.

with $a \approx 9.6$, i.e. much more than η of linear polymers with $a = 3.4$ as found comparing linear and star-shaped poly(isoprene) [17].

Thermal studies on LiCF_3SO_3 solutions in linear and star-shaped OEGE by DSC show pronounced melting peaks in the temperature range from -41 to -14 °C (temperature values are related to the minima of the melting peaks) in the case of the linear ether solutions indicating a high tendency to crystallization of the linear ethers (Fig. 2). Besides, a glass transition was detected for each ether at a temperature < -64 °C. In contrast to this, the crystallization of the star-shaped ethers in the solutions, with exception of OEGE-3 730, is completely suppressed, only glass transitions in the temperature range from -50 to -85 °C were detected.

The glass transition temperatures T_g increase with increasing molecular weight of the ethers because of the decreasing mobility of the ether molecules. In the case of OEGE-3 730, a melting peak was found whose intensity is considerably lower than that of the melting peaks found for the linear ethers. Moreover, the melting temperature T_m of -28 °C (T_m is based on the minimum of the peak) is distinctly lower than the melting temperature of the linear EG₁₁DME. Hence, the tendency to crystallization of OEGE-3 730 is strongly decreased.

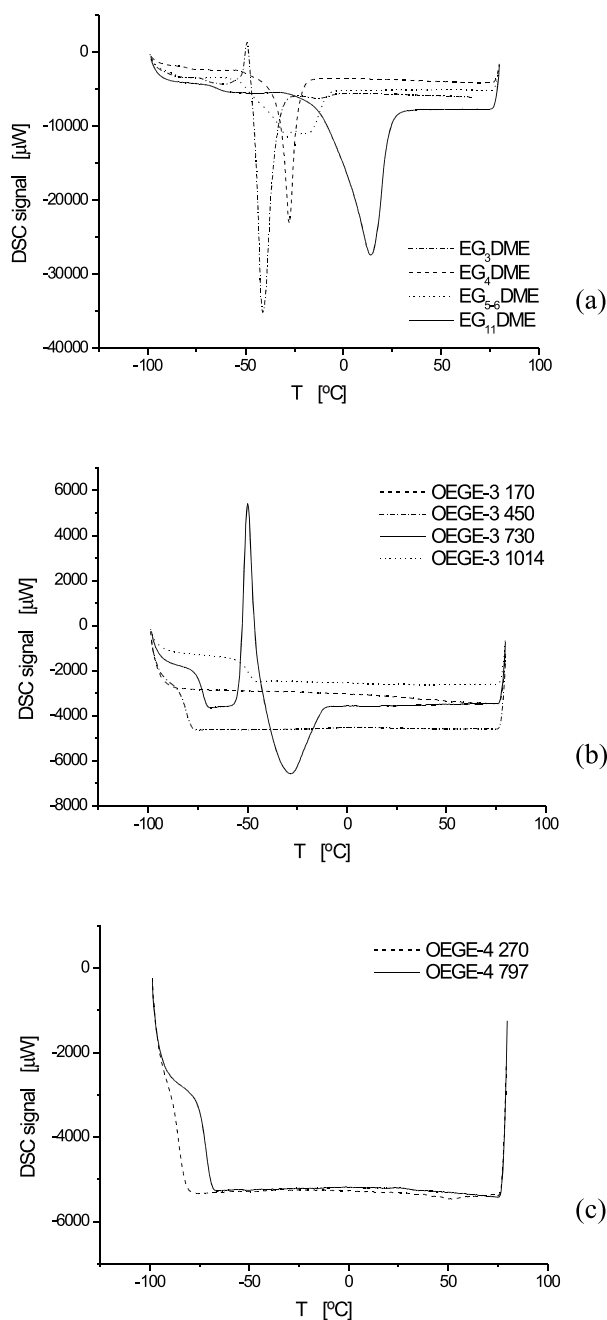


Fig. 2. DSC thermograms of solutions of linear and star-shaped OEGE with 0.55 mol/kg LiCF_3SO_3 .

3.2. Polymerization reactions

The course of the photoinitiated polymerizations was studied by means of photo-DSC measurements. The time t_{max} in which the maximum polymerization rate is reached, is given in Table 1 as a measure for the polymerization rate of the various systems studied.

It can be seen in Fig. 3, that the time t_{max} decreases, i.e. the polymerization rate is enhanced, with increasing viscosity of the plasticizer/salt solutions. That means, the polymerization is not influenced by the type of OEGE. The

Table 1
Influence of the architecture of OEGE and of the electrolyte LiCF_3SO_3 on the time t_{max} in which the maximum photopolymerization rate of EG_3DMA at 30 °C is reached

Plasticizer	wt%	$c_{\text{electrolyte}}$ (mol/kg)	t_{max} (min)
EG_{11}DME	69	0.55	0.57
OEGE-3 450	69	0.55	0.57
OEGE-3 730	55	0.55	0.31
	59	0.55	0.32
	64	0.55	0.38
	69	0.55	0.47
	69	0	0.68
OEGE-4 270	69	0.55	0.72
OEGE-4 797	69	0.55	0.50

linear variation of t_{max} with $\ln \eta$ corresponds to the well-known relationship between $1/k_t \sim \eta$ considering that $1/t_{\text{max}} \sim r_p \sim 1/k_t^{0.5}$ with k_t = termination rate constant, r_p = overall polymerization rate.

As can be seen in Table 1, the salt increases the polymerization rate as expected. This so-called salt effect was already often observed in free-radical polymerizations, e.g. of EG_{23}DMA in the presence of LiCF_3SO_3 [15]. It was explained by the interactions of the salt ions with the monomer and the propagating radicals, which weaken the repulsive dipole-dipole interactions between radicals and monomer and hence allow higher propagation rates.

As a further effect of the salt that increases the polymerization rate, the decrease of the termination rate due to the enhanced viscosity of the solutions (Fig. 1) may be assumed.

A decrease of t_{max} is observable when the content of the plasticizer OEGE-3 730 is reduced from 69 to 64 wt% (Table 1). However, a further reduction of the content of plasticizer to 55 wt% do not lead to a further decrease of t_{max} . This can be explained by the combination of two

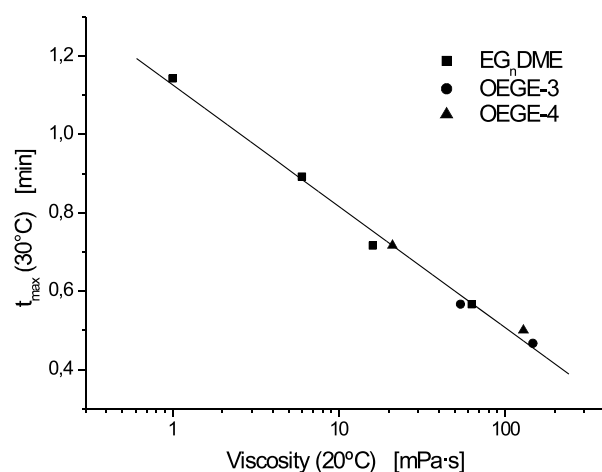


Fig. 3. Dependence of the time t_{max} , in which the maximum polymerization rate is reached, on the viscosity of the OEGE/ LiCF_3SO_3 solution (LiCF_3SO_3 content: 0.55 mol/kg, OEGE content of the monomer solution: 69 wt%).

opposite effects. On the one hand, the reduction of the plasticizer is connected with the increase of the concentration of the monomer EG₃DMA, what leads to a rise in the polymerization rate. On the other hand, the viscosity of the mixture is reduced because of the comparably low viscosity of EG₃DMA resulting in a decrease of the polymerization rate as described above.

As expected, the polymerization rate decreases with increasing content of the comonomer CyMA (Fig. 4) due to the reduced viscosity of the mixtures because of the low viscosity of CyMA, though the concentration of the methacrylate groups becomes somewhat higher due to the increasing concentration of CyMA ($M_{\text{CyMA}} = 125.13 \text{ g/mol}$, $M_{\text{EG}_3\text{DMA}} = 286.32 \text{ g/mol}$).

In all polymerizations, complete conversions of C=C double bonds were obtained as found by DSC. The calculation of the C=C conversion from the DSC data is described in Section 2. The analysis of the gels by Raman spectroscopy and of the sols (obtained by extraction of gels with chloroform) by ¹H NMR spectroscopy showed no reference to residual monomers.

3.3. Thermal transitions and dynamic thermo-mechanical properties of the gels and network density of the polymer matrix

The comparison of the DSC plots in the Figs. 2 and 5 shows, that the crystallization of OEGE-3 730 but also of the linear ethers is distinctly lower in the gels based on EG₃DMA than in the corresponding ether-salt solutions.

Accordingly, lower melting enthalpies (ΔH_m) were found for the gels (Table 2).

In the case of the homopolymer gel with 64 wt% OEGE-3 730, ΔH_m is very low implying that the crystallization of the ether is almost completely suppressed. Moreover, the melting and glass transition temperatures of the salt solutions in the gels are slightly higher than those of the salt solutions alone. The lower tendency to crystallization

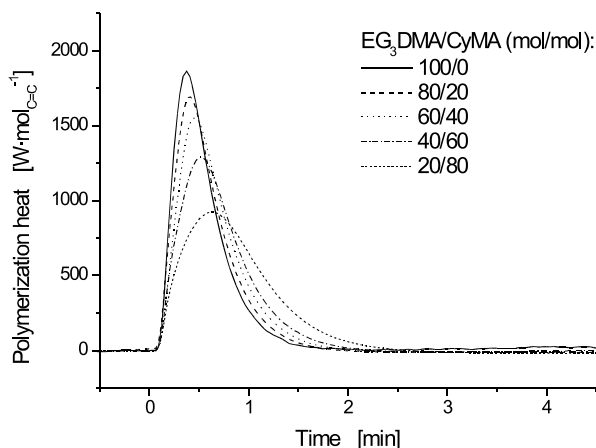


Fig. 4. Photopolymerization of EG₃DMA and CyMA in the presence of 64 wt% OEGE-3 730 and OEGE-4 797, respectively, and 0.55 mol/kg LiCF₃SO₃ initiated with 2 mol% Lucirin at 30 °C.

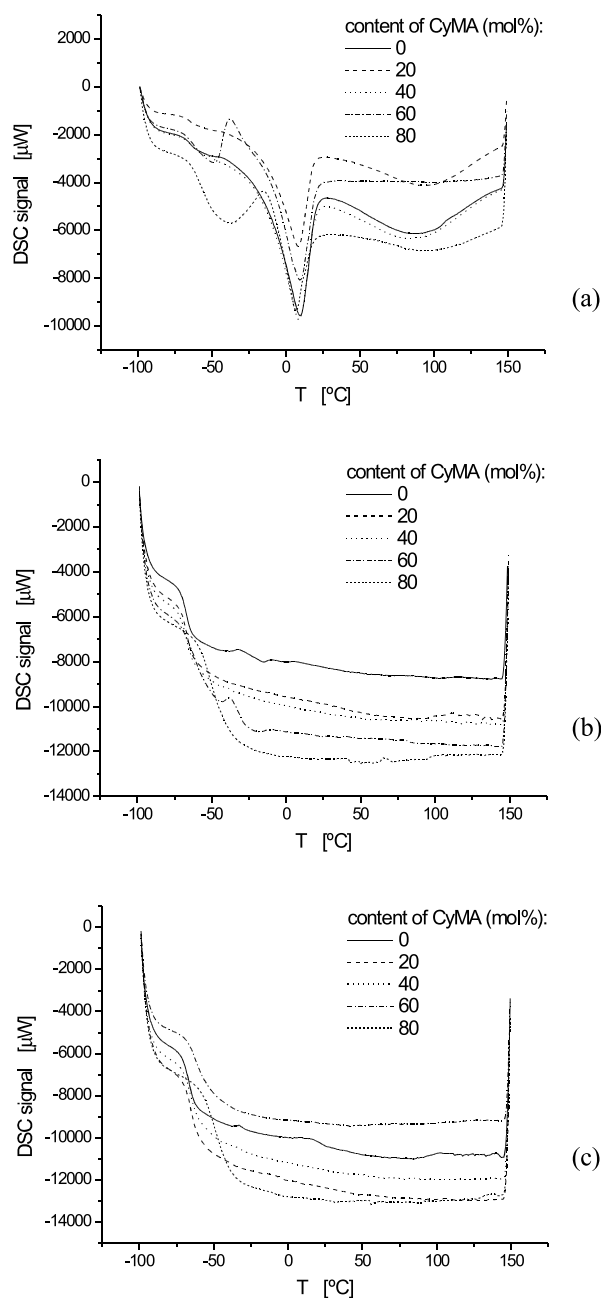


Fig. 5. DSC thermograms of poly(EG₃DMA-co-CyMA) gels including 64 wt% OEGE and 0.55 mol/kg LiCF₃SO₃, (a) plasticizer: EG₁₁DME, (b) plasticizer: OEGE-3 730, (c) plasticizer: OEGE-4 797.

of the ethers in the gels and also their higher T_g and T_m are caused by the reduced mobility of the ether molecules in the polymer network.

It was expected that the insertion of the polar comonomer CyMA into the polymer network results in a decrease of the network density owing to the lower content of the cross-linker EG₃DMA and consequently, in an enhanced mobility of the plasticizer molecules. On the contrary, increasing T_g for the star-shaped plasticizers OEGE-3 730 and OEGE-4 797 and decreasing ΔH_m of EG₁₁DME (Fig. 5, Table 2) indicate a reduction of the mobility of the ether chains with

Table 2

Glass transition temperature T_g , melting temperature T_m and melting enthalpy ΔH_m of linear and star-shaped oligo(ethylene glycol) ethers in poly(EG₃DMA-co-CyMA) based gel electrolytes and in solutions with LiCF₃SO₃ (LiCF₃SO₃ content in solutions and gels: 0.55 mol/kg, OEGE content in the gels: 64 wt%) determined by DSC

Content of CyMA in poly(EG ₃ DMA-co-CyMA) (mol%)	$T_{g,OEGE}$ (°C)	$T_{m,OEGE}^a$ (°C)	$\Delta H_{m,OEGE}^a$ (mJ/mg)
Plasticizer: EG ₁₁ DME			
0	−65	10	79
20	−65	8	81
40	−65	8	71
60	−60	10	54
80	−54	7	22
EG ₁₁ DME/salt solution	−64	−14	126
Plasticizer: OEGE-3 730			
0	−67	−15	1
20	−67	−	−
40	−67	−	−
60	−60	−18	2
80	−49	−	−
OEGE-3/salt solution	−73	−28	33
Plasticizer: OEGE-4 797			
0	−67	−	−
20	−65	−	−
40	−64	−	−
60	−61	−	−
80	−48	−	−
OEGE-4/salt solution	−72	−	−

^a T_m is based on the minimum of the melting peak, ΔH_m is related to the ether mass.

increasing CyMA content. This behaviour could be based on the increasing homogeneity of the networks with increasing CyMA content. The latter was already observed for poly(EG₃DMA-co-CyMA) networks plasticized with EG₁₁DME [6].

The gels were also studied by dynamic thermo-mechanical analysis (DMA) to detect glass transitions of the polymer matrix, which could not be observed by the DSC measurements, and to evaluate their mechanical stability. In the compression modulus, $\tan \delta = E''/E'$ (δ = phase angle between applied stress and resulting strain, E'' = loss modulus and E' = storage modulus) and E' were determined in dependence on the temperature.

Fig. 6 shows the DMA plots for gels with EG₁₁DME, OEGE-3 730 and OEGE-4 797 as plasticizer. At temperatures between approximately 80 and 155 °C, there appears a maximum of $\tan \delta$ for all gels marking the glass transition temperature T_g of the polymer (T_g for all gels see Table 3). Additional maxima at low temperatures characterize the glass transition and/or the melting of the plasticizer corresponding to the DSC results. The existence of several maxima of $\tan \delta$ in a curve shows that the gels are generally heterogeneous materials consisting of highly cross-linked, low swollen regions and of low cross-linked, strongly swollen regions.

Analogous to the results obtained by DSC, the T_g of the star-shaped plasticizers OEGE-3 730 and OEGE-4 797 increase with increasing CyMA content of the copolymers indicating a reduction of the mobility of the ether chains.

However, it has to be noticed, that in the case of EG₁₁DME, no tendency of T_g and T_m to higher temperatures was found by DMA (Table 3). Moreover, T_g of the copolymers decrease with increasing CyMA content to values widely

Table 3

Glass transition temperature T_g of the copolymer matrix and T_g and melting temperature T_m of linear and star-shaped oligo(ethylene glycol) ethers in poly(EG₃DMA-co-CyMA) gels (OEGE content: 64 wt%, LiCF₃SO₃ content: 0.55 mol/kg) determined by DMA

Content of CyMA in poly(EG ₃ DMA-co-CyMA) (mol%)	$T_{g, Polymer}$ (°C)	$T_{g, OEGE}$ (°C)	$T_{m, OEGE}$ (°C)
Plasticizer: EG ₁₁ DME			
0	141	−	0
20	136	−20	13
40	113	−24	7
60	88	−	−
80	80	−32	−
Plasticizer: OEGE-3 730			
0	146	−48	−20
20	153	−61	−
40	130	−58	−
60	103	−47	−
80	101	−36	−
Plasticizer: OEGE-4 797			
0	138	−44	−
20	143	−45	−
40	130	−36	−
60	102	−	−
80	92	−23	−

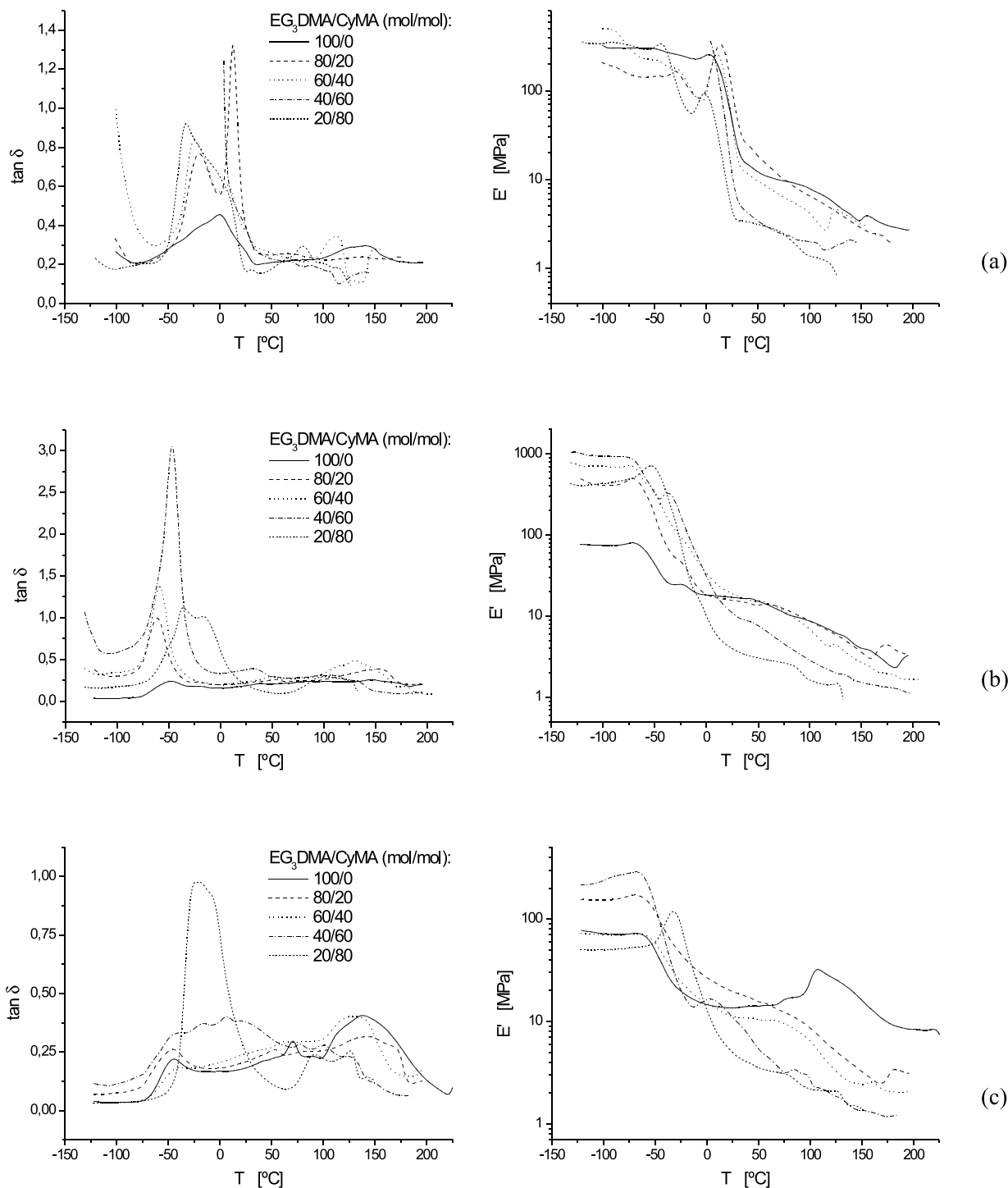


Fig. 6. DMA plots of poly(EG₃DMA-*co*-CyMA) gels including 64 wt% OEGE and 0.55 mol/kg LiCF₃SO₃, (a) plasticizer: EG₁₁DME, (b) plasticizer: OEGE-3730, (c) plasticizer: OEGE-4797.

below the T_g of poly(CyMA) of 122 °C, which can be explained by the increasing plastication of the stronger cross-linked regions of the copolymers indicating that the copolymer network are more evenly swollen. The results obtained by DMA show clearly, that the network structure becomes more homogeneously with increasing CyMA content in the presence of EG₁₁DME as well as in the

presence of star-shaped plasticizers as concluded from the DSC results.

As can be seen in Fig. 6, the course of the E' curves is dependent on the type of the plasticizer. With increasing temperature, E' decreases in the range of the found T_g and T_m of the ether, in the case of EG₁₁DME only in the range of T_m because of the higher tendency to crystallization of the

ether. Owing to its comparatively high T_m , E' and therewith the mechanical strength of the gels decreases in the presence of EG₁₁DME only at higher temperatures than in the presence of the star-shaped ethers. As can be seen from E' above 25 °C in Fig. 6, the mechanical strength of the gels becomes lower with increasing CyMA content of the copolymer matrix due to the decreasing network density.

This is a result of the decreasing content of the cross-linker EG₃DMA, mentioned above. It is characterized by the enlargement of the molecular weight M_c of the chains between the network junction points. However, in previous investigations by DMA, higher M_c values were reached than expected in the case of completely extracted copolymers synthesized from EG₃DMA and CyMA in the presence of EG₁₁DME [6], which was explained by occurrence of intramolecular cyclization reactions during the polymerization and incorporation of plasticizer molecules into the polymer network. It is visible in Fig. 7, that the M_c values of the networks also determined by DMA on basis of completely extracted gels show a stronger increase with rising CyMA content in the case of copolymers which had been synthesized in the presence of star-shaped plasticizers.

However, the sol–gel analysis did not indicate any incorporation of plasticizer into the network. Therefore, it is assumed that the stronger increase of M_c in the presence of star-shaped plasticizers is the result of cyclization reactions occurring with increasing probability.

3.4. Ionic conductivity

Fig. 8 shows, that the ionic conductivity σ of the gels containing OEGE-3 730 and OEGE-4 797, respectively, is slightly lower than σ of the gels containing EG₁₁DME in the temperature range of 15–60 °C as found for the corresponding salt solutions. This is explicable with the worse solvation behaviour of star-shaped OEGE ($M < 1000$ g/mol) for Li⁺ ions as observed by us by Raman spectroscopic measurements [18].

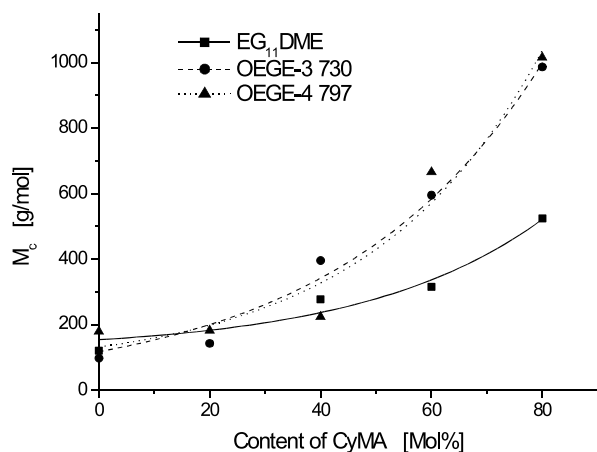
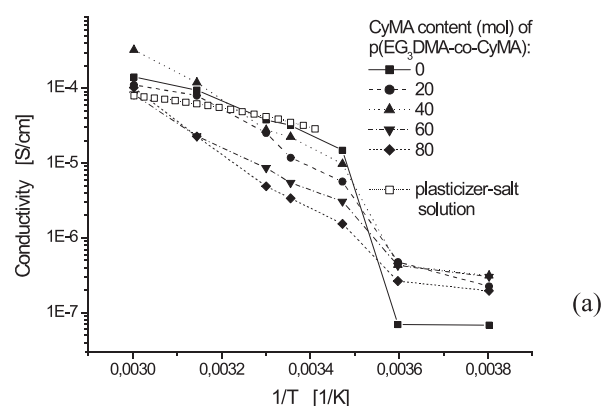
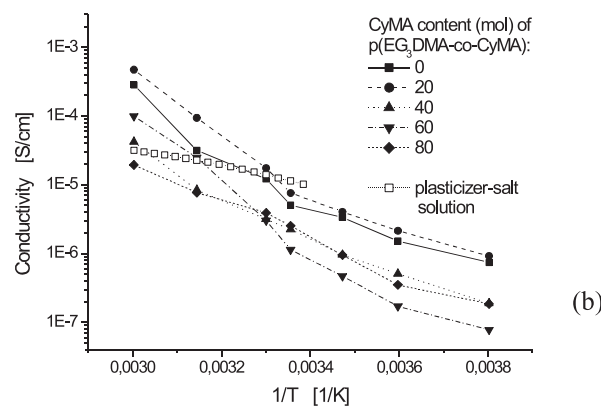


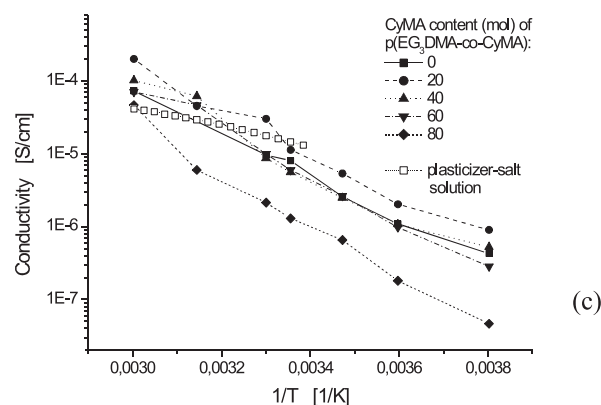
Fig. 7. Dependence of the average molecular weight M_c of the chains between the network junction points on the CyMA content of the polymer matrix.



(a)



(b)



(c)

Fig. 8. Ionic conductivity σ of poly(EG₃DMA-co-CyMA) gels including 64 wt% OEGE and 0.55 mol/kg LiCF₃SO₃ compared with σ of the corresponding OEGE/LiCF₃SO₃ solutions, (a) plasticizer: EG₁₁DME, (b) plasticizer: OEGE-3 730, (c) plasticizer: OEGE-4 797.

However, the conductivity of the gels with EG₁₁DME is reduced considerably at temperatures < 15 °C because of the crystallization of the ether. Below room temperature, the gels have a lower conductivity than the corresponding salt solutions (Fig. 8), but σ of the gels increases stronger with increasing temperature than that of the salt solutions. This means, the ionic conductivity of the gels is influenced by the polymer. Its stronger increase is based on the enhanced

mobility of the polymer chains. However, the higher conductivity of the gels than that of the corresponding salt solutions found at temperatures $>30\text{ }^{\circ}\text{C}$ may be attributed to the different instruments (Section 2.11: conductometer for the solutions and impedance spectrometer for the gels) used for the measurements.

At higher CyMA contents, the conductivity is decreased. This behaviour corresponds with the reduced mobility of the plasticizer molecules at higher CyMA contents as detected by DSC and DMA.

4. Conclusions

Star-shaped oligo(ethylene glycol) methyl ethers (OEGE) for use as plasticizers in polymer gel electrolytes can be prepared by methylation of commercially available ethoxylates from trimethylol propane and pentaerythrit with methyl iodide and potassium hydroxide in dioxane. It requires a two-step procedure to attain methylation degrees $>95\%$. Yields of 40–80% are obtainable after purification of the lower molecular products by distillation and of the higher molecular products by column chromatography.

The star-shaped OEGE exhibit somewhat lower viscosities than the linear ones. Solutions of the ion conducting salt LiCF_3SO_3 in OEGE show both for linear and star-shaped OEGE nearly the same dependence of the viscosity on the molecular weight up to $M \approx 800\text{ g/mol}$. This seems as an upper limit of M for use of star-shaped OEGE as a plasticizer, because an extraordinarily high increase in the viscosity was observed for the three arm OEGE with $M = 1056\text{ g/mol}$ (OEGE-3 1014) and its salt solution in agreement with results obtained for linear and star-shaped poly(isoprene) [17].

The rate of the photoinitiated polymerization of tri(ethylene glycol) dimethacrylate (EG_3DMA) and its copolymerization with the polar comonomer cyanomethyl methacrylate (CyMA) in the presence of OEGE and LiCF_3SO_3 , as studied by DSC measurements, increases in the same way with increasing viscosity of the linear and star-shaped OEGE.

The essential advantage of star-shaped OEGE for use as a plasticizer in gel electrolytes compared with linear OEGE is their distinctly lower tendency to crystallize, which is even completely suppressed in the gels in the most cases studied. Whereas the ionic conductivity of solutions and gels with star-shaped plasticizers is slightly lower than that with linear ones at temperatures above room temperature, the strong

decrease of the conductivity by crystallization of the linear plasticizer below room temperature does not occur with star-shaped plasticizers.

Acknowledgements

The financial support by the Bundesministerium für Wirtschaft (BMWi) and the VARTA Microbattery GmbH is gratefully acknowledged.

References

- [1] Hikmet RRM, Michels I. *Adv Mat* 2001;13(5):338.
- [2] Claude-Montigny B, Rioteau E, Lemordant D, Topart P, Bosser G. *Electrochim Acta* 2001;47(4):533.
- [3] Caillon-Caravanier M, Claude-Montigny B, Lemordant D, Bosser G. *Solid State Ionics* 2002;149(3,4):275.
- [4] Morita M, Tanaka A, Yoshimoto N, Ishikawa M. *Solid State Ionics* 2002;152–153:161.
- [5] Sandner B, Weinkauff A, Reiche A, Siury K, Tübke J, Wartewig S, Shashkov S. *Electrochim Acta* 1998;43:1263.
- [6] Reiche A, Sandner R, Weinkauff A, Sandner B, Fleischer G, Rittig F. *Polymer* 2000;41:3821.
- [7] Sandner B, Tübke J, Werther A, Sandner R, Wartewig S, Shashkov S. *Electrochim Acta* 1998;43:1563.
- [8] Sandner B, Reiche A, Siury K, Weinkauff A, Kotzian N, Sandner R, Tübke J, Wartewig S. *Batterien von den Grundlagen bis zur Anwendung*. In: Kruger FJ, Russow J, Sandstede G, editors. GDCH-Monographie, vol. 12. Frankfurt: a.M. Heinz Spengler GmbH; 1997.
- [9] Reiche A, Tübke J, Siury K, Sandner B, Fleischer G, Wartewig S, Shashkov S. *Solid State Ionics* 1996;85:121.
- [10] Reiche A, Tübke J, Sandner R, Werther A, Sandner B, Fleischer G. *Electrochim Acta* 1998;43:1429.
- [11] Tabuchi M, Miura K, Nakamura S, Wada Y., *JP* 2002063813, 2002 (CA 136:223262).
- [12] Ueda M, Suzuki T. *J Polym Sci, Polym Chem Ed* 1983;21:2997.
- [13] Leonard J. Heats and entropies of polymerization, ceiling temperatures, equilibrium monomer concentrations, and polymerizability of heterocyclic compounds. In: Brandrup J, Immergut EH, Grulke EA, editors. *Polymer handbook*. New York: Wiley; 1999. p. II/369.
- [14] Weinkauff A., *Dissertation*, Universität Halle-Wittenberg; 1999.
- [15] Sandner B, Kotzian N, Tübke J, Wartewig S, Lange O. *Macromol Chem Phys* 1997;198:2715.
- [16] McLeish TCB, Milner ST. *Adv Polym Sci* 1999;143:195 and references therein.
- [17] (a) Pearson DS, Mueller SJ, Fetters, LJ. *ACS Polym Prepr* 1982;23(2):21.
(b) Elias HG. *Makromoleküle*, 6th ed *Physikalische Strukturen und Eigenschaften*, vol. 2. Weinheim: Wiley-VCH; 2001 p. 503.
- [18] Edelman K, Sandner B. *Solid State Ionics* 2004;170:225.